Soils and Foundations 2015;55(5):1015–1029

HOSTED BY

ELSEVIER

CrossMark

The Japanese Geotechnical Society

Soils and Foundations

www.sciencedirect.com
journal homepage: www.elsevier.com/locate/sandf

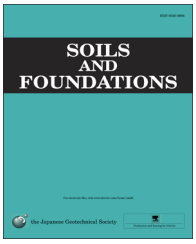

Report on a reconnaissance survey of damage in Kathmandu caused by the 2015 Gorkha Nepal earthquake

Mitsu Okamura[a,*], Netra P. Bhandary[a], Shinichiro Mori[a], Narayan Marasini[a], Hemanta Hazarika[b]

[a]*Graduate School of Science and Engineering, Ehime University, Japan*
[b]*Faculty of Engineering, Kyushu University, Japan*

Received 29 July 2015; received in revised form 14 August 2015; accepted 18 August 2015
Available online 4 October 2015

Abstract

Nepal was hit by the M7.8 Gorkha earthquake on April 25, 2015, which was the largest earthquake in Nepal's history since 1934. The recent report presented by the Government of Nepal indicates that the recorded death toll has reached about 8800.

Following the earthquake, the Japanese Geotechnical Society (JGS), Asian Technical Committee of ISSMGE on Geotechnical Natural Hazards (ATC3), Japan Society of Civil Engineers (JSCE) and Japan Association for Earthquake Engineering (JAEE) decided to jointly dispatch a survey team to Nepal to conduct a reconnaissance survey of the major damage caused by the earthquake. This report summarizes the results of the survey of the geotechnical and structural damage in the Kathmandu valley, which were observed by the survey sub-team between May 1 and 8, 2015. Geotechnical and geological characteristics of a deep soil profile up to 600 m and a shallow profile up to 30 m are also described with the help of the database system established by Bhandary et al. (2012). In order to study the correlation between building damage ratios and the predominant period of ground vibration, a partial exhaustive type survey was conducted along NS line where microtremor measurements had been previously conducted in 2008. The predominant period of ground vibration was short at the ridge of the valley and long at its center, ranging from 1.2 to 4.5 s. A total of 532 buildings were assessed and more than 90% were classified as "No damage" or "Negligible to slight Damage" (Grade 0 and Grade 1), whereas only 5% of buildings were assessed as "Substantial to heavy damage" to "Destruction" (Grade 3 to Grade 5).

Five locations were identified where the soil had liquefied. Liquefaction-induced damage to structures at these locations was not found, except at Nepal Engineering College where minor settlement of the college building was observed. During the 1934 earthquake, foundation liquefaction was observed in Tundhikhel area, but in the 2015 earthquake no evidence of liquefaction was detected in this area.

The Kathmandu–Bhaktapur Road of Araniko Highway was heavily damaged in the Lokanthali area. The subsidence of soft soils and their lateral spreading in this area may have exacerbated the damage to this road.

Keywords: Gorkha Nepal earthquake; Earthquake damage survey; Natural frequency; Liquefaction; Road embankment

1. Introduction

Nepal was hit by the M7.8 Gorkha earthquake (epicenter: Barpak, Gorkha district, Fig. 1) on April 25, 2015 (Saturday, 11:56 AM local time). It was the largest earthquake in Nepal's history since 1934. Unlike past events, this earthquake has been followed by a large number of aftershocks, some of

*Corresponding author.
E-mail addresses: okamura@cee.ehime-u.ac.jp (M. Okamura), netra@ehime-u.ac.jp (N.P. Bhandary), mori@ehime-u.ac.jp (S. Mori), narayanmarasini@gmail.com (N. Marasini), hazarika@civil.kyushu-u.ac.jp (H. Hazarika).
Peer review under responsibility of The Japanese Geotechnical Society

http://dx.doi.org/10.1016/j.sandf.2015.09.005

which were as large as past damaging earthquakes in the region. As indicated in Fig. 1, more than 200 aftershocks had been recorded in the area about 200 km east of main shock epicenter by the time of the preparation of this paper. As seen in Fig. 1, the extent of the distribution of the aftershocks probably indicates the rupture zone, which has an effective width of approximately 80 km. The town of Barpak, at the epicenter of the earthquake, is situated about 80 km northwest of Kathmandu, the capital of the country.

The recent report presented by the Government of Nepal (GoN, 2015) indicates that the recorded death toll has reached about 8800 while the number of injured people is over 22,000. A district-wise distribution of the human casualties and injuries is shown in Fig. 2. The total death toll in the Kathmandu valley, where an estimated 4 to 5 million people including unregistered residents are supposed to have been living, has remained well below 2000 whereas the highest death toll of 3440 occurred in the Sindhhupalchowk district (population about 300,000). The highest numbers of injured people have been in the Kathmandu valley, accounting for nearly two-thirds of the total injured. As shown in Fig. 2, the human casualties and injuries have a greater concentration in the rupture zone districts from Gorkha in the west to Dolakha in the east.

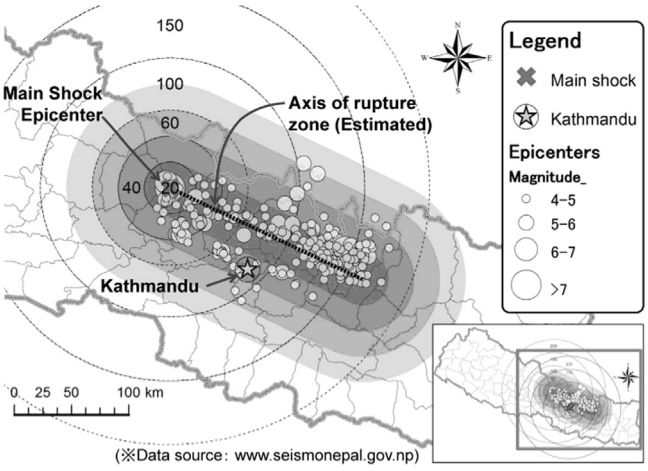

Fig. 1. Epicenter of 2015 Nepal Gorkha Earthquake and distribution of aftershocks.

A district-wise building damage distribution map is shown in Fig. 3. According to GoN (2015), the total number of completely damaged buildings and houses is now over 511,000; this number stands at about 75,000 in the Kathmandu valley alone. The highest number of rural and urban houses damaged completely is in Sindhupalchowk district (total houses/buildings about 67,000); here, the damage rate stands at 96% (fully damaged). The number of partially damaged houses and buildings in the affected districts is slightly less than 300,000 while in the Kathmandu valley alone it is close to 60,000. Consistent with the distribution of human casualties, the concentration of house/building damage is seen to be higher in the rupture zone districts.

According to a recently submitted post-disaster need assessment (PDNA) report by the National Planning Commission to the Prime Minister of Nepal, the total economic loss in 15 different sectors (Fig. 4) has been estimated to be about US $ 7 billion and the estimated reconstruction cost is about US$ 6.2 billion. The highest economic loss has been in the building structures and human settlements sectors, which show nearly half the total economic loss. This indicates that these are the most important sectors that needs to be strengthened against the effects of future earthquake disasters in Nepal.

Following the earthquake on April 25, 2015, the Japanese Geotechnical Society (JGS), Asian Technical Committee of ISSMGE on Geotechnical Natural Hazards (ATC3), Japan Society of Civil Engineers (JSCE) and Japan Association for Earthquake Engineering (JAEE) decided to jointly dispatch a survey team headed by Dr. Kiyota (University of Tokyo) to Nepal to conduct a reconnaissance survey of the major damage caused by the earthquake. This report summarizes the results of the survey of geotechnical and structural damage, which were observed in the Kathmandu valley by a survey sub-team between May 1 and 8, 2015.

2. Tectonics and historical earthquakes

The record of historical earthquakes in the Nepal Himalaya dates back to the 13th century, but no clear documentation of the damage that occurred is available in the literature. Tabulated data

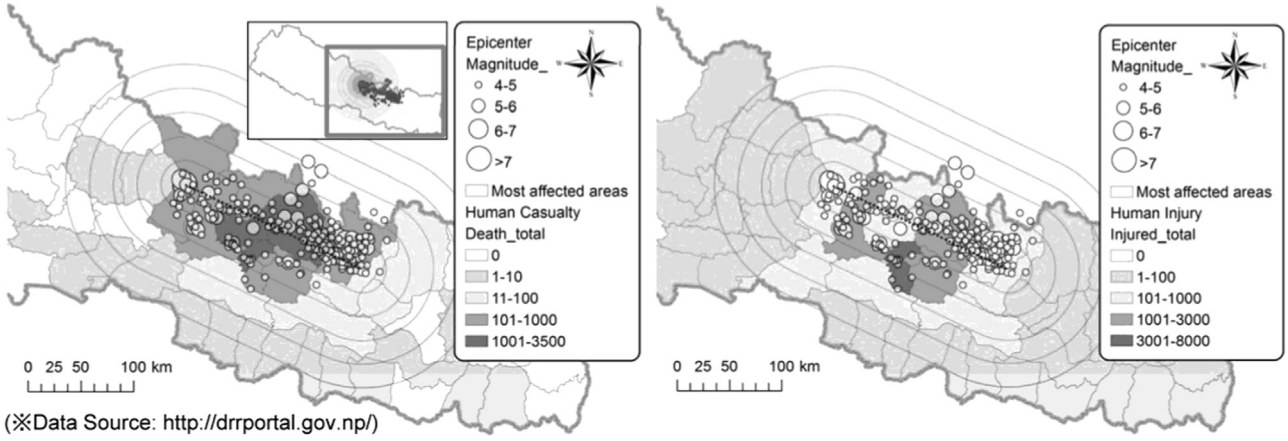

Fig. 2. District-wise distribution of human casualty and injured people.

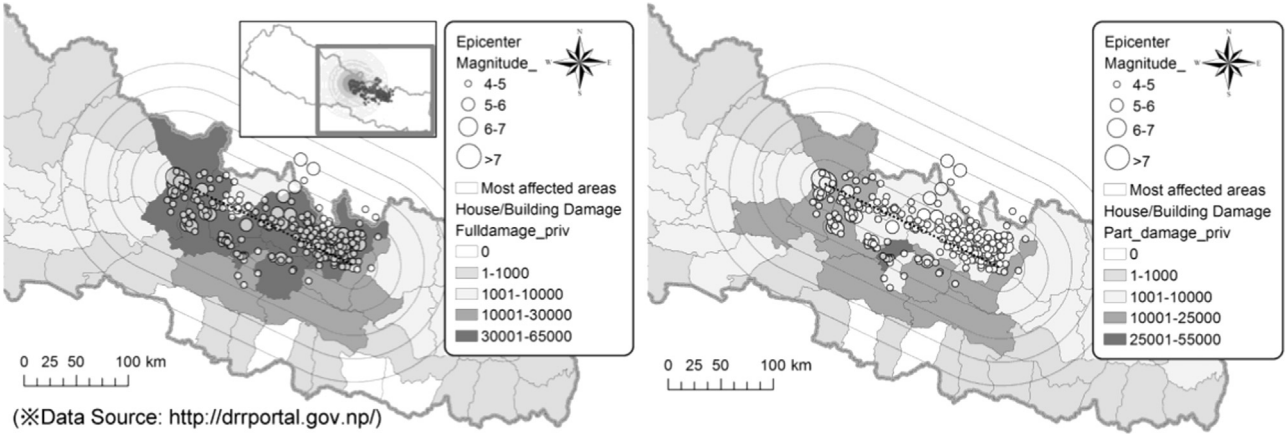

Fig. 3. District-wise building/house damage distribution map.

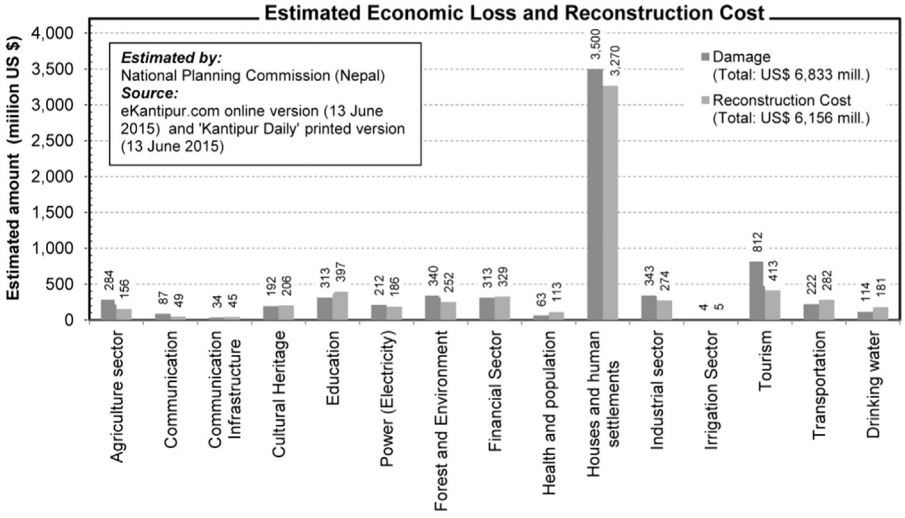

Fig. 4. Economic loss and reconstruction cost estimation (National Planning Commission, Nepal).

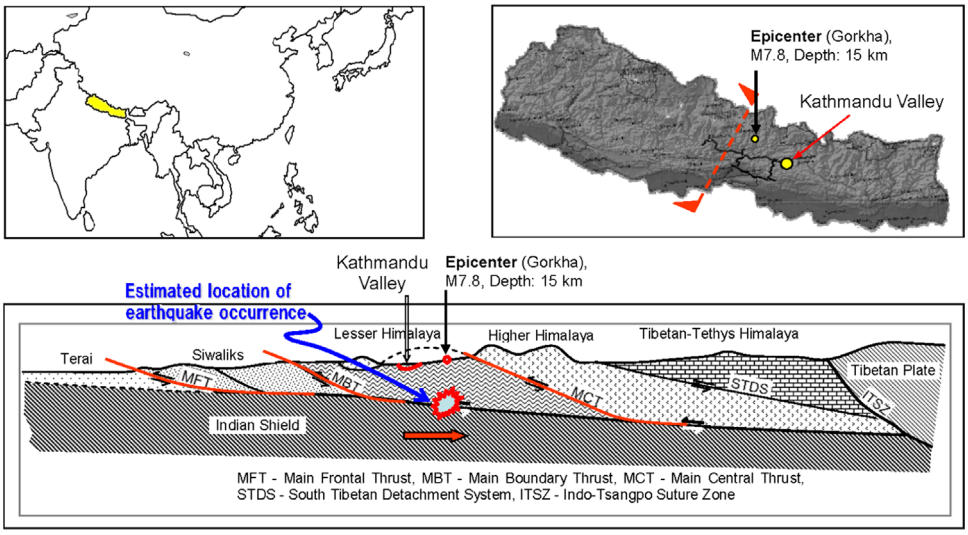

Fig. 5. The Indian plate subduction underneath the Eurasian plate and major thrust faults in the Himalaya region (cross-section adopted from Dahal (2005)).

on the historical earthquakes in Nepal and peripheral areas, as compiled by NSET and GHI (1999), indicate that a large earthquake occurs in the Nepal Himalaya roughly every 100 years. Since the last large earthquake in 1934 (i.e., Bihar–Nepal Earthquake, M8.1), 81 years have passed and it was widely estimated that a large earthquake was going to occur in the Nepal Himalaya within 100 years from 1934. During the last 35 years, three heavily damaging earthquakes and several damaging earthquakes have occurred in Nepal. The heavily damaging earthquakes include the 1980 far western region earthquake (M6.5, Darchula; MoHA et al., 2009), the 1988 eastern Nepal earthquake (M6.5, Udayapur; MoHA et al., 2009), and the 2011 earthquake (M6.9, Nepal–India border, USGS, 2011) while damaging earthquakes of $<$M6.0 were recorded almost every year from 1993 until 2003. In addition, there is a long list of minor earthquakes that occur almost every month in and around the Nepal Himalaya. These earthquake data indicate that Nepal is situated in a highly earthquake-prone plate tectonic zone of the Himalayas.

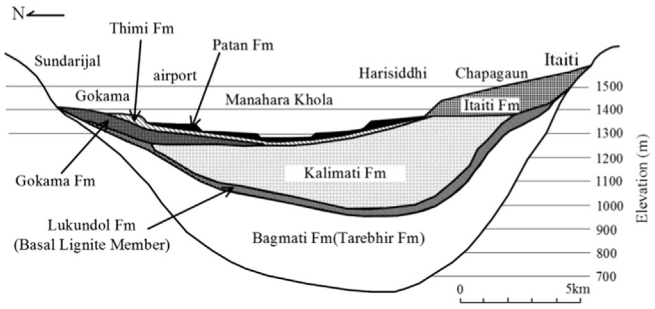

Fig. 6. Schematic geological cross section of the basin showing stratigraphic relationship of each formation (after Sakai, 2001).

The occurrence of earthquakes in the Himalayan region is primarily due to the collision between the Indian plate and the Eurasian plate (sometimes also referred to as the Tibetan plate in local or regional scale). As indicated in Fig. 5, the Indian plate moves northward and subducts underneath the Eurasian plate creating a zone of plate-tip squeezing at the Himalayas. This plate movement has resulted in the formation of the Himalayan mountains, the uplift of which occurs at an estimated rate of 2 cm per year (Bilham et al., 1995). Moreover, the area-wide compression and uplift of the Himalayan region has resulted in extensive distribution of regional and local faults. Some of these faults generate major earthquakes,

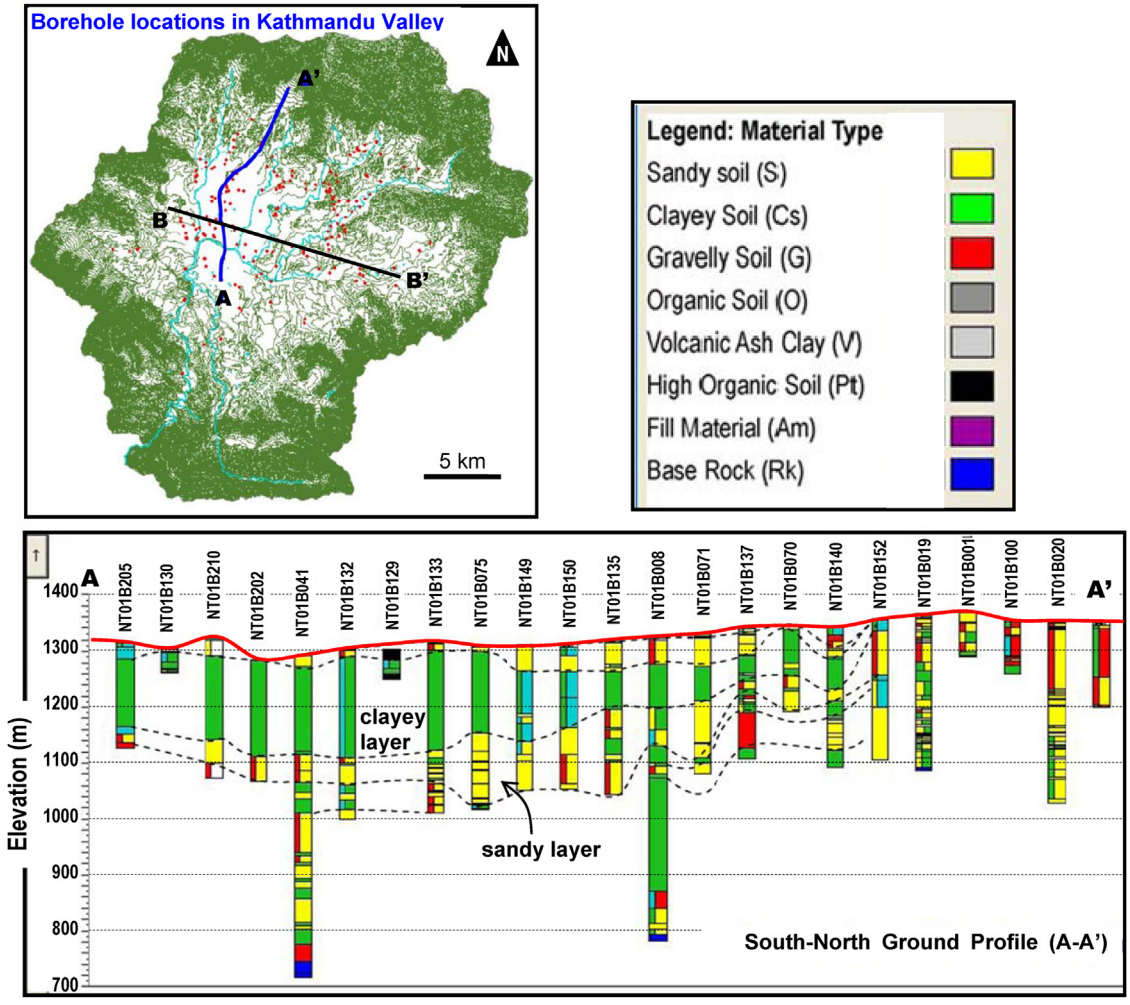

Fig. 7. Cross section of the basin showing geotechnical condition.

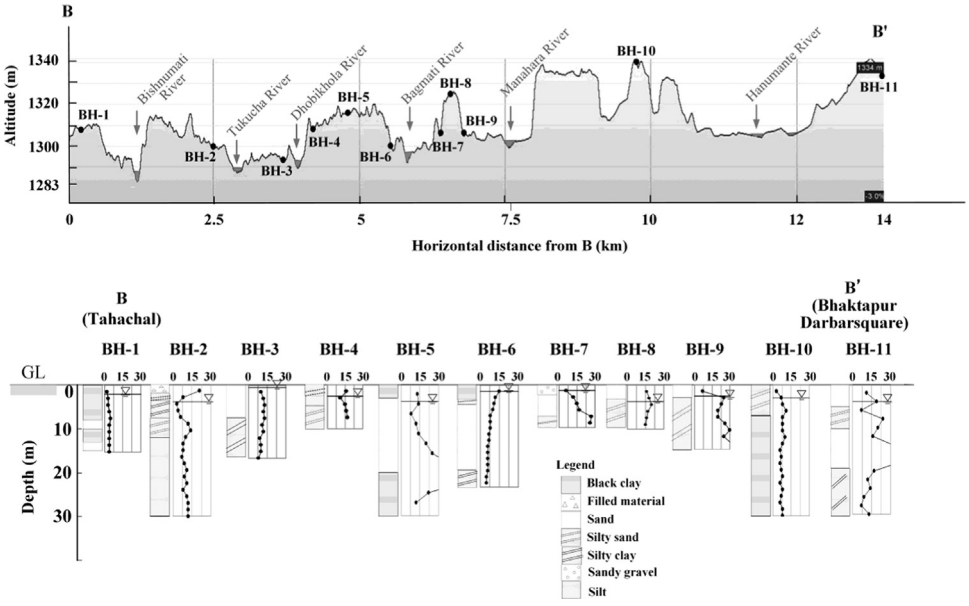

Fig. 8. Surface topography and boring data in a east–west section.

such as the 2008 Sichuan Earthquake during which nearly 88,000 people died. So far, however, the major earthquakes in and around the Nepal Himalaya have been mostly generated at the subduction zone of the Indian plate underneath the Eurasian plate (Fig. 5). The depth of the Gorkha Earthquake has been estimated to be about 15 km, which makes it clear that this earthquake was generated exactly at the depth of subduction plane. The exact mechanism involved in the generation of this earthquake is yet to be revealed, but a general interpretation is that the strain energy stored in the rupture zone due to the northward gently inclined thrust of the Indian plate was released with slipping of Eurasian plate-tip below the Main Boundary Thrust (MBT; Fig. 5).

Banerjee and Bürgmann (2002), Bettinelli et al. (2006), Bilham and Szeliga (2008), among others, mentioned that the Himalayan region contracts under the influence of Indian plate subduction at a rate of 16–18 mm/year. About 100 years of devastating earthquake history in the Himalayan region indicates that the region was hit by four major earthquakes in 1897, 1905, 1934, and 1950 (Bilham et al., 1995; Chander, 1988, 1989; Khattri, 1987, 1992; Molnar, 1990; Molnar and Pandey, 1989; Pandey et al., 1995; Seeber et al., 1981; Seeber and Armbruster, 1981), but no earthquake of this scale had ever occurred in the central part of the Himalaya. Khattri (1987) identified this part as a seismic gap in the Himalayan region, and Bilham et al. (1995), Pandey et al. (1995) also mentioned that it was and still is the highest potential location for the next major earthquake in the Himalayan region. It was from this time that most researchers working in seismicity in the Himalayan Front consolidated their anticipation that a major earthquake was going to occur in central Nepal within 80–100 years of the 1934 Bihar–Nepal Earthquake.

The location of the 2015 Gorkha Earthquake leads most researchers to conclude that it is probably the anticipated central seismic gap earthquake, but the eastward shifting (i.e., the directivity) trend of almost all the aftershock occurrences (Fig. 1) also puts a question mark over this understanding. This has led to a speculation that occurrence of yet another major earthquake, probably much larger than the Gorkha Earthquake, in this region within the next 10–20 years is inevitable. According to an estimation made by the JICA (2002) study, the fatal loss of lives in the Kathmandu valley alone in a 1934 scenario earthquake could exceed 40,000, a large number of building structures in the valley could be completely damaged, and most lifeline infrastructures including hospital and school buildings could be left unusable for several weeks. In contrast, however, not only the human casualties in the valley have been less but the damage to building structures has also been much less than anticipated.

Fig. 9. Microtremer measurement arrangement along two lines across Kathmandu Valley, NS Line and EW Line (after Kukidome et al., 2009).

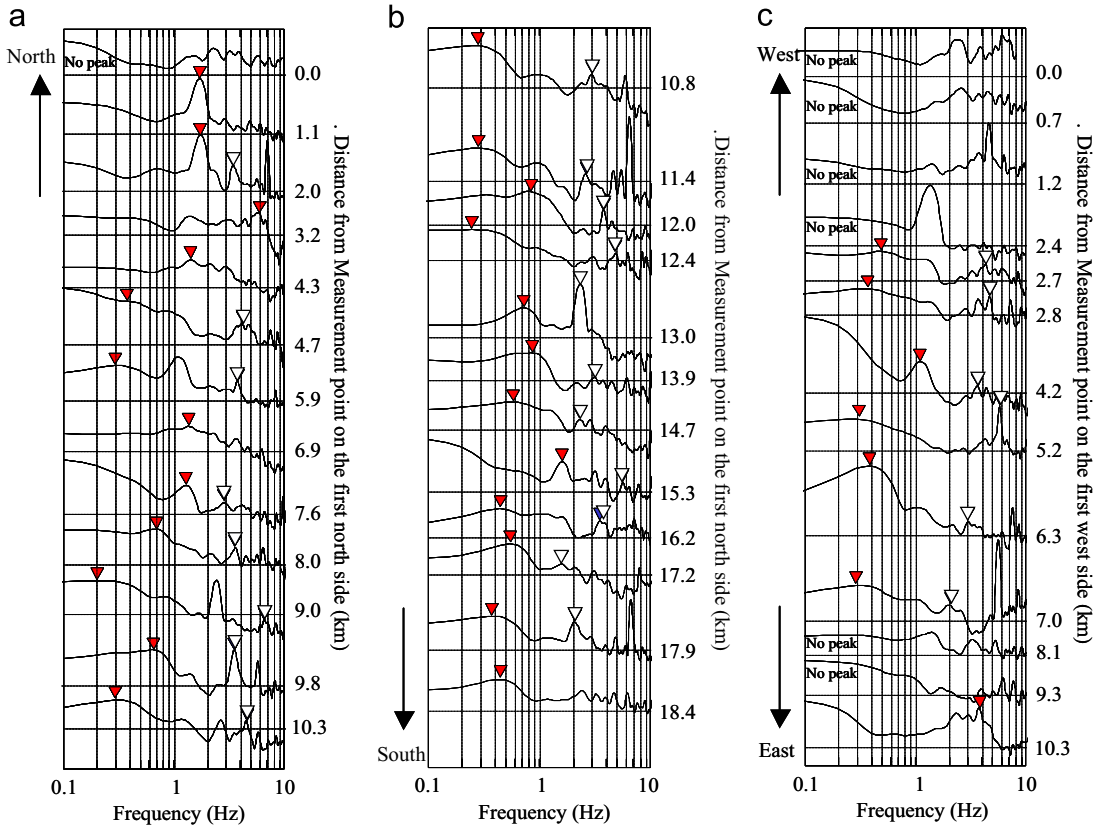

Fig. 10. Sequential arrangement of HV spectral ratios at all the measurement points (a)(b) along NS Line, and (c) along with EW Line (after Kukidome et al., 2009).

Although the vibration pattern of the Kathmandu valley deposits seems to have been very different from that during the 1934-scenario earthquake, it is surprising to most investigators to note that the damage has been incomparably less than estimated.

It is worth mentioning that, among the major earthquakes in the recorded history of the area, the Bihar–Nepal Earthquake of 1934 (Ambraseys and Douglas, 2004; Hough and Bilham, 2008) with a maximum intensity of X-MMI (i.e., an intensity of X in Modified Mercalli Intensity system) caused extensive damage in the Kathmandu valley (Dunn et al., 1939; Pandey and Molnar, 1988). The total number of deaths in whole Nepal was 8519, with 4296 of these in the valley itself. This earthquake destroyed about 19% of the buildings in the valley and damaged about 38% of them (Pandey and Molnar, 1988; Rana, 1935). The level of destruction was particularly severe in Bhaktapur City in the eastern part of the valley (Pandey and Molnar, 1988; Rana, 1935). Many historic temples and monuments also collapsed or sustained severe damage. Sand boils were observed in a central district of Kathmandu city.

3. Geotechnical conditions of the Kathmandu valley

The main sources of the sediments in the basin of the Kathmandu valley are the surrounding mountains from where the sediments were carried by an ancient drainage system. The study based on the available borehole logs concluded that the sediment distribution in the valley is not uniform and divided into three main parts: the Bagmati formation, the Kalimati Formation and the Patan Formation as indicated in Fig. 6 (Sakai, 2001). The section shown is for the eastern part of the valley running from Sundarijal in the north to Itaiti village in the south.

Bhandary et al. (2012) have prepared a geo-information database of the Kathmandu valley. They have selected about 300 logs from a total of about 700 existing logs of boreholes in the Kathmandu valley. As not all borings were carried out for geotechnical investigation purposes most of them had only soil profile depths and no geotechnical property information. The database system gives approximate ground profiles through any desired line connecting a set of borehole locations. The locations of the 300 boreholes, their data and soil profiles in cross section A–A′ are presented in Fig. 7. Some of them are as deep as 600 m from ground surface and extend to the bed rock. The section runs from Syuchatar (North) to Bhaktapur (South) through the central district of Kathmandu. Sand and gravel deposits are dominant in the north and clay layers tend to be thicker in the south.

Fig. 8 shows the surface topography and shallow geotechnical conditions in a WE section (cross section B–B′) which crosses from Tahachal in the west and Bhakatapur Durbar Square in the east and runs through the center of the city. Major rivers running through the valley also lie within this section. The maximum and minimum elevations are 1342 m

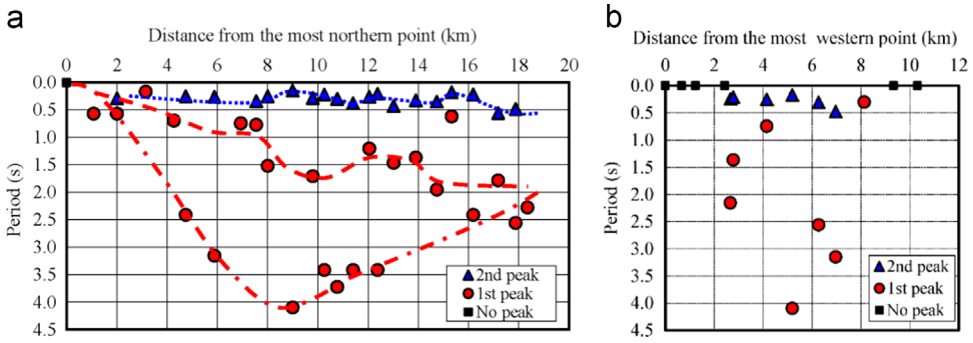

Fig. 11. Distribution of predominant period of ground (after Kukidome et al., 2009). (a) along NS line (b) along EW line.

and 1283 m, respectively. The 11 borehole logs of shallow depth ranging 10–30 m in the section show detailed information about SPT N values, soil types and the location of the ground water table. The sediments near the rivers (BH-2, 3, 4 and 6) mainly consist of sand and silt with a shallow ground water table, typically 1–3 m from the ground surface. The SPT N values are mostly lower than 15. In the westernmost borehole near Tahachal (BH-1), the black clayey soil deposits extend from the surface to a depth of 15 m. At Tribhuvan International Airport (BH-7, 8 and 9) sandy gravel, coarse to medium sand, and silty sand are the major soil types. In this area the soils exhibits relatively higher SPT N values of >15 below the ground water table. The borehole near Thimi Bhaktapur (BH-10) indicated mostly a clay layer with a thickness greater than that encountered in other boreholes. The borehole located at Bhaktapur Durbar Square (BH-11) indicated mainly coarse to fine sand strata down to 19 m from the surface, which is then underlain by clayey silt. The geotechnical characteristics at shallower depth may be summarized as follows: the soil stratification of the deposit is highly heterogeneous; the ground water table is shallow in all bore holes, typically at 1–3 m below ground level; and SPT N values are not high.

4. Evaluation of the natural period vibration and structural damage

4.1. Microtremor measurement

Microtremor measurements were conducted at night during November, 2008 along two lines across the Kathmandu valley, a north–south line (NS Line) and an east–west line (EW Line), as shown in Fig. 9 (Kukidome et al., 2009). The NS Line starts at Pasikot, runs southward through Lazimpat, Thamel, Tripreshwar, Teku, Kopundol, Phulchowk, crosses the Ring Road at Jawalakhel, and finally approaches southern Chasikot. The EW Line starts at a hillside temple in the west of Swayambhunath, runs eastward through Kimdol, crosses the Vishnumati River, extends along the north end of Ratna Park and finally reaches Gauchar.

Fourier analysis was conducted for each velocity–time history segment extracted from raw data in terms of stable time ranges and the horizontal to vertical spectral ratio (HV spectral ratio) was calculated. The sequential arrangement of HV spectral ratios of the north–south component at all the measurement points along the NS line and the EW line is shown in Fig. 10. Most of the HV spectral ratios have two predominant frequencies, the lower one corresponds to amplification through sediments overlying the bedrock of the Kathmandu Basin and the upper one corresponds to amplification in the surface deposits.

The HV spectral ratios of the northernmost point on the NS line and three westernmost points on the EW line, which are located on a hill area, show no predominance. Since a no-predominance or flat HV spectral ratio means a site with no amplification due to surface wave generation, these sites can be regarded as a type of bed rock outcrop in terms of the dynamic amplification of earthquake ground motion. Except for these points, each HV spectral ratio has two predominant frequencies ranging between 0.2 and 0.5 Hz or 0.7 and 1.5 Hz in the lower frequency range, and from 2 to 6 Hz in the higher frequency range. Similar tendencies were observed in the EW components. The predominant period of ground vibration at the sites was calculated with the averaged predominant frequencies of the NS and EW components and are shown in Fig. 11. The spatial distribution of the predominant period can be understood to be roughly representative of the basin profile as shown in Fig.6. On the NS line, a gradual change from 2.5 to 4.5 s and another gradual change from 1.2 to 2.0 s are found in Fig. 11(a). The longest predominant period was at 9 km from the north end of the line and this point corresponds to the north-west corner of Ratna Park, 0.9 km from the north-east of Durbar Square. In addition, the distribution of the predominant period from 0.2 to 0.5 s seems to become longer from north to south. On the other hand, along EW line, the central part of the line has somewhat longer predominant frequencies.

4.2. Relationship between ground natural frequency and structural damage

(1) Dynamic properties of buildings in Kathmandu

In this section, we focus on damage to buildings in the Kathmandu valley. Three- to six-story residential and office buildings built in reinforced concrete with infilled

Fig. 12. Typical buildings assessed. (a) six-story RCIW residential building that suffered Grade 1 damage. (b) three-story brick URM houses that suffered Grade 4 damage.

walls (RCIW) are dominant in the Kathmandu valley, while two-story unreinforced masonry (URM) houses secondarily dominant. Photographs of typical buildings are depicted in Fig. 12. Moreover, high-rise apartments with not less than 10 stories have also been recently built there. The natural period of a building can be estimated using an empirical formula for RCIW buildings shown in the Nepal Building Code for seismic design, NBC 105 (GoN, 1994). As per the code, the natural period of a building varies from 0.3 to 0.6 s for a 3–6 story building while it varies from 0.8 to 1.3 s for 10–17 story building.

(2) Rapid damage assessment of buildings

In order to study correlation between damage ratio and predominant period of ground vibration, the authors carried out a partial exhaustive type survey along the NS Line. Eight members of the team were divided into four groups. Each group had a Nepali member for guiding and interviewing purposes.

Damage assessment of buildings was conducted in accordance with the European Macroseismic Scale 1998 (EMS-98, European Seismological Commission, 1998), which has been used mainly for damage assessment of masonry buildings. The dominant types of buildings are unreinforced masonry (URM) buildings and reinforced concrete frame-filled brick buildings

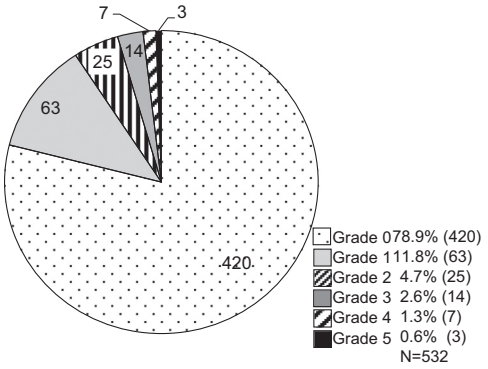

Fig. 13. Result of rapid damage assessment.

and structures, which are not familiar to Japan. Damage assessment as per EMS-98 would be beneficial in the compilation of damage assessment carried out by different institutes from different countries.

The results of the assessment as per EMS-98 can be converted to the assessment scale issued by the Architectural Institute of Japan and the Japan Building Disaster Prevention Association. EMS-98 classifies building damage into six grades as follows;

Grade 0: no damage
Grade 1: negligible to slight damage (no structural damage, slight non-structural damage).
Grade 2: moderate damage (slight structural damage, moderate non-structural damage).
Grade 3: substantial to heavy damage (moderate structural damage, heavy non-structural damage).
Grade 4: very heavy damage (heavy structural damage, very heavy non-structural damage).
Grade 5: destruction (very heavy structural damage).

Fig. 13 shows the provisional results of the rapid damage assessment. A total of 532 buildings were assessed and more than 90% of them were classified as having “no” or “negligible to slight damage” (Grades 0 and 1) while the percentage of buildings assessed as having “substantial to heavy damage” to “destruction” (Grades 3–5) was only about 5%.

Fig. 14 shows the distribution of buildings assessed using six grades of damage. It is not easy to see any systematic change along the NS assessment line, but the severely damaged area is located in the central part of the line, which is almost equivalent to the central part of the NS Line of microtremor measurement.

A denser distribution in a broader area may be needed for detailed investigation of the correlation between building damage and natural period of ground vibration.

5. Soil liquefaction

Because the Kathmandu valley deposits are composed mainly of saturated sand and clay layers with a shallow ground water table, liquefaction is highly anticipated. Fig. 15

depicts the liquefaction susceptibility map prepared by the United Nation Development Programme for an M7.8 scenario earthquake and a peak ground acceleration of approximately 0.3 g (UNDP, 1994). Liquefaction susceptibility was judged "high" and "medium" in a large area along the major rivers.

The authors tried extensively to identify the liquefied area from 3 May until 7 May. Because no news of liquefaction had practically been reported on TV and newspapers until then, the authors visited many places where the liquefaction susceptibility is high and medium. Meanwhile SNS was utilized to collect information. The following five locations shown in Fig. 15 were identified to have liquefied. Liquefaction-induced damage to structures in these areas was not found except in the case of the Nepal Engineering College (L4) where buildings suffered subsidence. All these areas are in the high or medium liquefaction susceptibility zone with the exception of Jharuwarashi area (L1).

(1) Jharuwarashi area (L1)

Jharuwarashi is located in the southeast part of the Kathmandu valley, and the Karmasasa River originates near this area. On the right bank of Karmasasa River, ground fissuring of approximately 100 m long and 10 cm

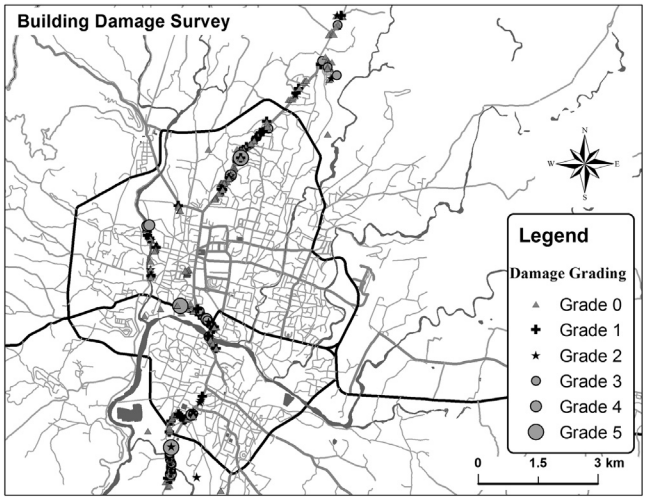

Fig. 14. Distribution of buildings assessed into six Grades.

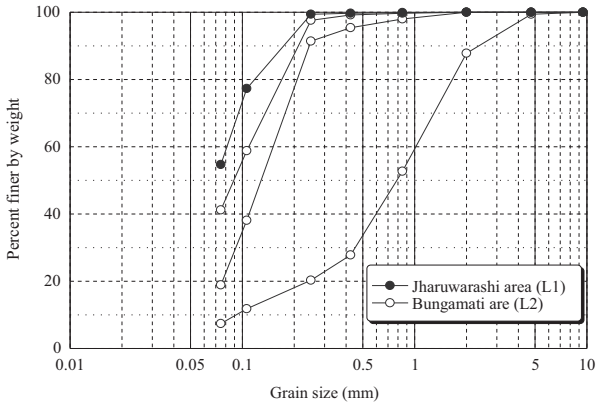

Fig. 16. Grain size distributions of erupted sand.

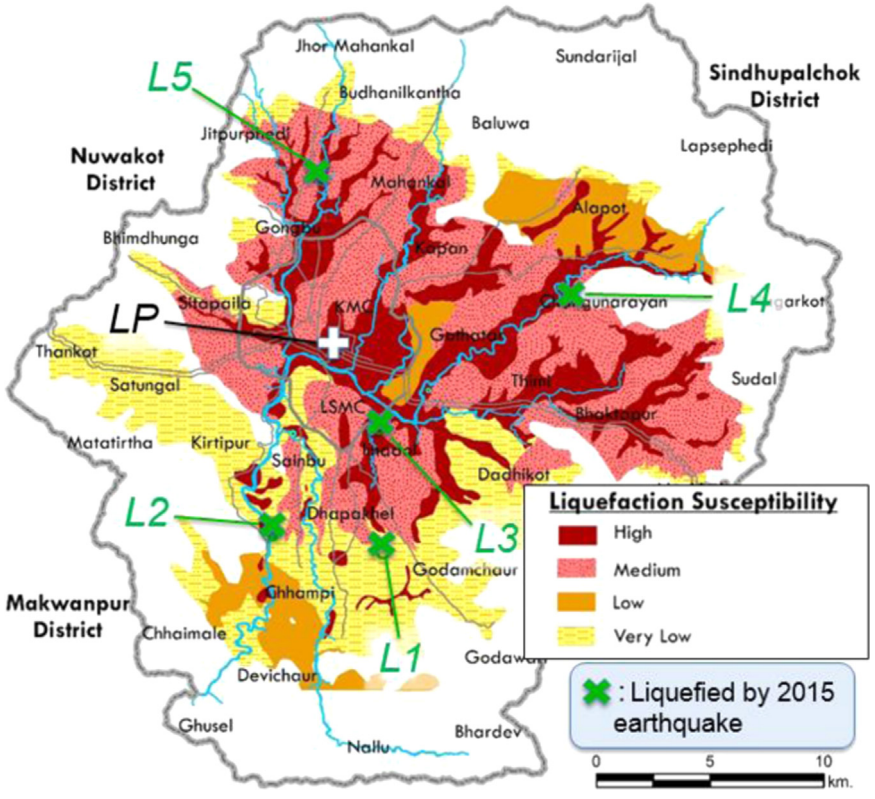

Fig. 15. Liquefaction susceptibility map prepared by UNDP (1994) together with identified locations of liquefaction by the 2015 earthquake.

wide was observed. Sand boils were ejected through the fissures. The fissures were parallel to the river, indicating the soil to be laterally spreading towards the river. The ejected soil was fine sand containing 50% non-plastic silt, as shown in Fig. 16.

(2) Bungamati area (L2)

Extensive soil liquefaction occurred in the Bungamati area. This area located in the flood area of the Bagmati River and is used as fields for growing two crops of rice and wheat annually. A large number of sand volcanos were detected in this area, approximately 300 m long and 200 m wide (Fig. 17). The ejected soil was coarse to fine sand with 5–40% non-plastic silt, as shown in Fig. 16. Fissures with openings up to 15 cm wide were also detected the directions of which were mostly parallel to the river.

(3) Imadol area (L3)

On the right bank of the Karmasasa River, small-size sand boils were detected in vegetable fields approximately 100 m from the river. This area was indicated to be a zone of moderate liquefaction vulnerability, however, no damage was induced by liquefaction to nearby buildings and lifeline facilities.

(4) Nepal Engineering College (L4)

Extensive liquefaction occurred at the Nepal Engineering College located on the left bank of the Monahara River. A flat plain extends approximately 700 m wide along the river channel between river terraces in this neighborhood. Sand boiling and fissures occurred as shown in Fig. 18 and the college buildings subsided slightly.

(5) Manamaiju area (L5)

The Manamaiju area is located on the north-west of Kathmandu valley and the Bishnumati River runs through this area. On the right bank of the Bishnumati River, some sand boils were found in paddy fields (Fig. 19).

X-ray diffraction analyses were conducted on sands erupted at liquefaction sites of L1 and L2 to assess their mineralogy. It was found that quartz, feldspar, mica and calcite are the dominant minerals. The relative amount of minerals in the sands determined by the integrated intensity ratio were quartz 60–80%, feldspar 10–20%, mica 10–20% and calcite 5–10%. Mica mineral grains have an impacts on the cyclic properties of sand as the liquefaction resistance and volumetric change

Fig. 18. Erupted sand at Nepal Engineering College (L4).

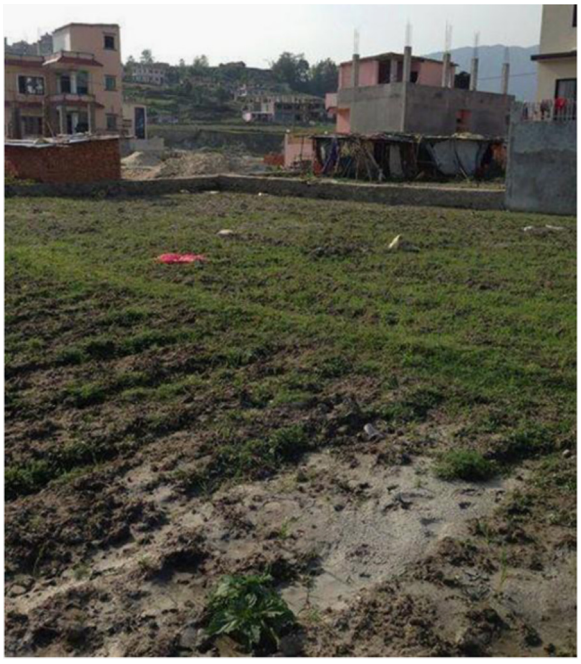

Fig. 19. Erupted sand at Manamaiju area (L5).

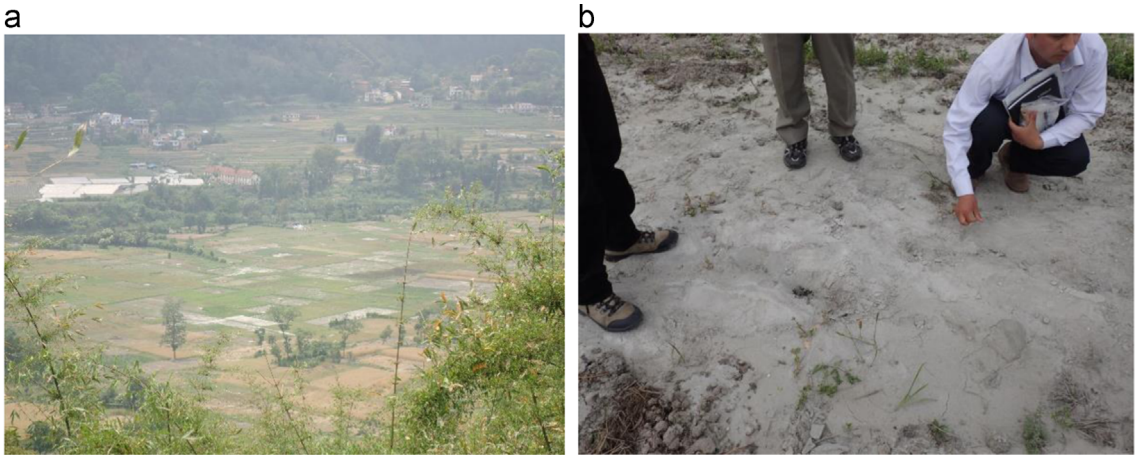

Fig. 17. Erupted sand boils at Bungamati (L2). (a) overview of the area (b) erupted sand.

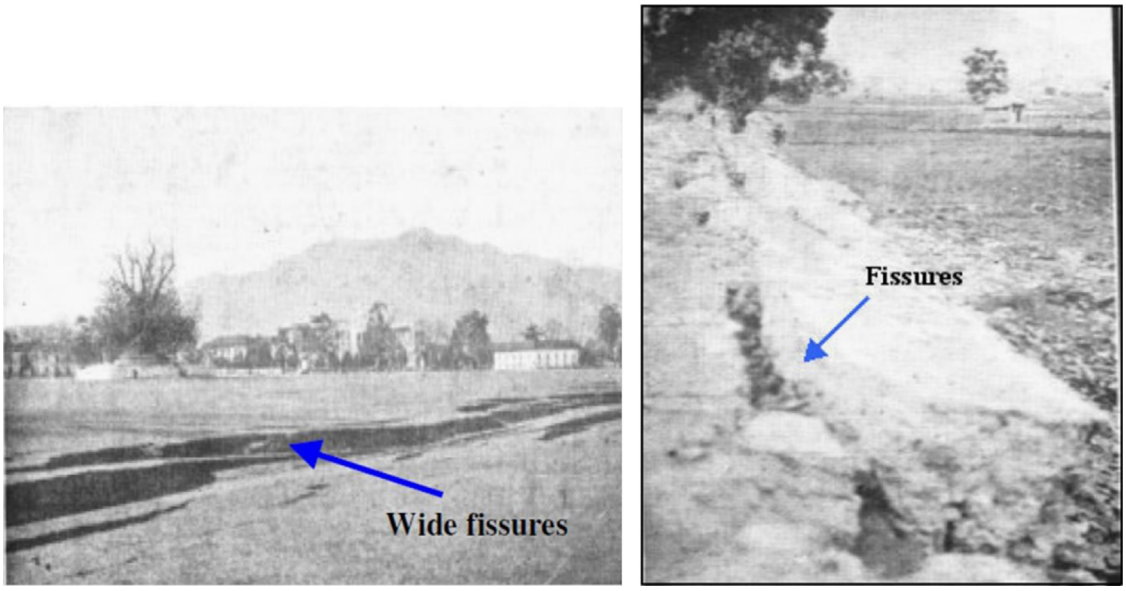

Fig. 20. Liquefaction in Tundhikhen area (labeled "LP" in Fig. 14) by the 1934 earthquake (after Rana, 1935).

characteristics. The liquefaction resistance and the in-situ penetration resistance of the mica-rich sand of Kathmandu need to be further studied in order to validate the empirical method to assess liquefaction susceptibility.

Rana (1935) reported the occurrence of widespread liquefaction in the valley during the Bihar Nepal earthquake in 1934. The Tundhikhel area (labeled "LP" in Fig. 15) was severely fissured and the ejection of liquefied sand occurred, as shown in Fig. 20. Although that earthquake occurred in the dry season (January 15, 1934), most of the paddy fields and roads in the area were flooded by ejected sand boils. In the Tundhikhel area located at the center of the city, the current ground surface is mostly covered with buildings and pavement but there is a large open space remaining, the old parade ground, which has turned into a tent-city for the evacuees right after the earthquake. No evidence of liquefaction caused by the 2015 earthquake was detected in this area.

6. Damage to the Kathmandu–Bhaktapur Road

The 9.142 km segment of the Kathmandu–Bhaktapur Road section of the Araniko Highway was upgraded by expanding the previous two-lane road to four lanes through JICA (Japan International Cooperation Agency) funded project. The road is also known as the Nepal–Japan Friendship Road. The Kathmandu–Bhaktapur Road is designed to serve not only as a road to ensure the smooth transportation of goods and people between Kathmandu and Bhaktapur, but also to play an important role in linking the Kathmandu Valley with the Eastern Terrain via the Araniko Highway and the Sindhuli Road (which connects Dhulikhel–Sindhuli–Bardibas with the East–West Highway). Furthermore, this road section has also improved the connection of the Kathmandu valley with the north via the Araniko Highway.

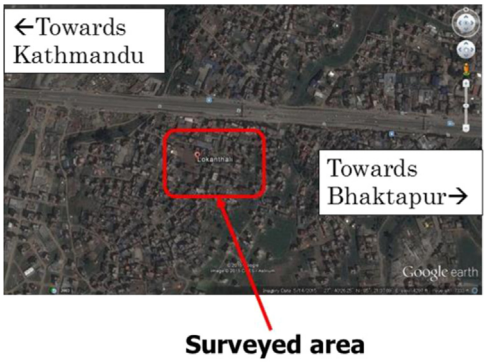

Fig. 21. Kathmandu–Bhaktapur road (URL source: http://www.earth.google.com).

This is a vital part of the physical infrastructure for Nepal in terms of connectivity to China and India (JICA, 2007). A part of this road was damaged during the Gorkha Earthquake. This section summarizes the damage to the road and the surrounding infrastructures during the earthquake as well as the geological and geotechnical information available close to this area.

Our survey focused only on the damaged part of the road located near the Lokanthali area (Fig. 21), covering a length of about 400 m. The state of the road before and after the earthquake is shown in Fig. 22. The various locations, types and extent of damage of the surveyed area are shown in Fig. 23. On the Kathmandu side, heaving and subsidence of the road, slope failures in the main road and access road, ground fissuring, retaining wall damage and damage to the residential buildings close to the access road were observed. Similarly, on the Bhaktapur side, heaving and subsidence of the main road, slope failures in the access road and ground fissuring were observed.

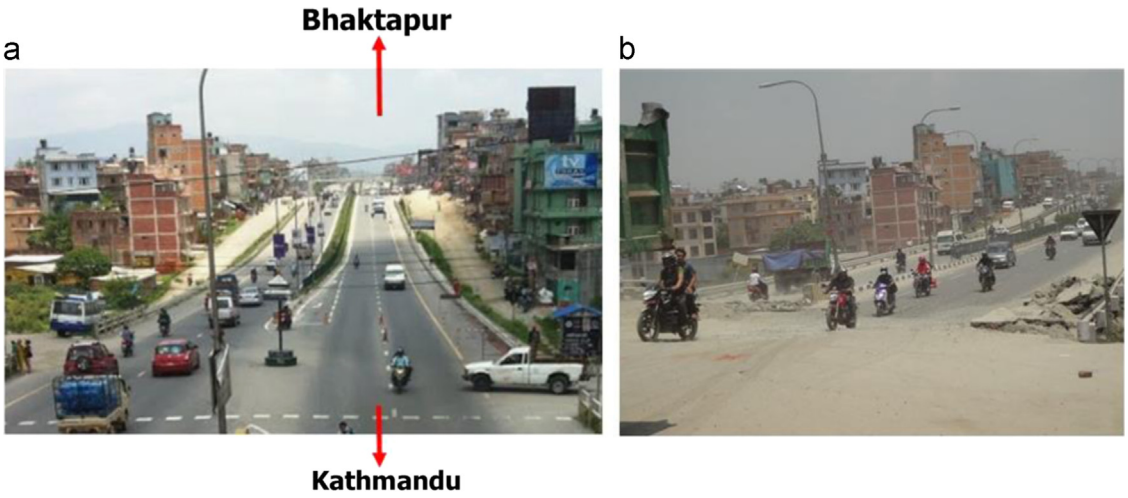

Fig. 22. State of the road before and after the earthquake. (a) Before the Eq. (b) After the Eq.

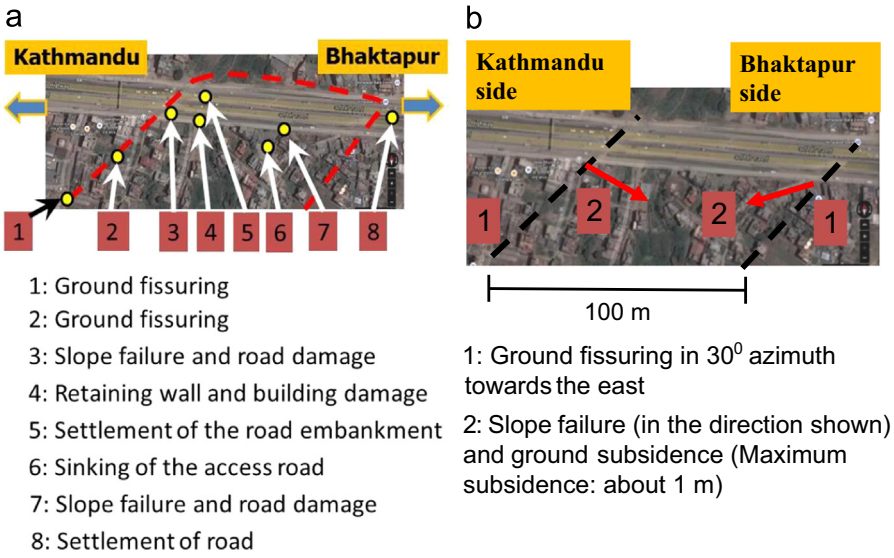

Fig. 23. Locations of the damaged area in the main road and the access road (source map URL: http://www.maps.google.com).

Slope failure at Location 3 is shown in Fig. 24. As seen in the figure the traffic police box was tilted by about 12 degrees due to slope failures and settlement of the road. On the Bhaktapur side (Location 7) similar slope failure also took place in the access road (Fig. 25 a) and subsidence of the main road was also observed (Fig. 25b). In Location 5, huge settlement of the access road on the Kathmandu side was observed (Fig. 26a). An apartment building close to this subsiding road was found to have settled and tilted as seen in Fig. 26b. At Location 4, there are two types of retaining walls: one is a reinforced retaining wall and the other is a gravity retaining wall. As seen in Fig. 27, in the joint between the two walls damage was observed. In addition, in some parts of the gravity retaining wall, cracks were observed along the same line in which ground fissuring of the access road was observed. Ground fissuring extended up to the residential areas along the road. Two residential buildings located along this fissure were found to be heavily damaged (Fig. 28). According to the owner of the building, whom the authors met during the investigation, the building settled by more than 1 m towards the Kathmandu–Bhaktapur road, and consequently tilted due to differential settlement

Fig. 24. Slope failure in the Kathmandu side.

Fig. 25. Slope failure and subsidence (Bhaktapur side). (a) Sinking of the main road and (b) slope failure in the access road.

Fig. 26. Access road and building damage (Kathmandu side). (a) Subsidence of the access road and (b) tilted building.

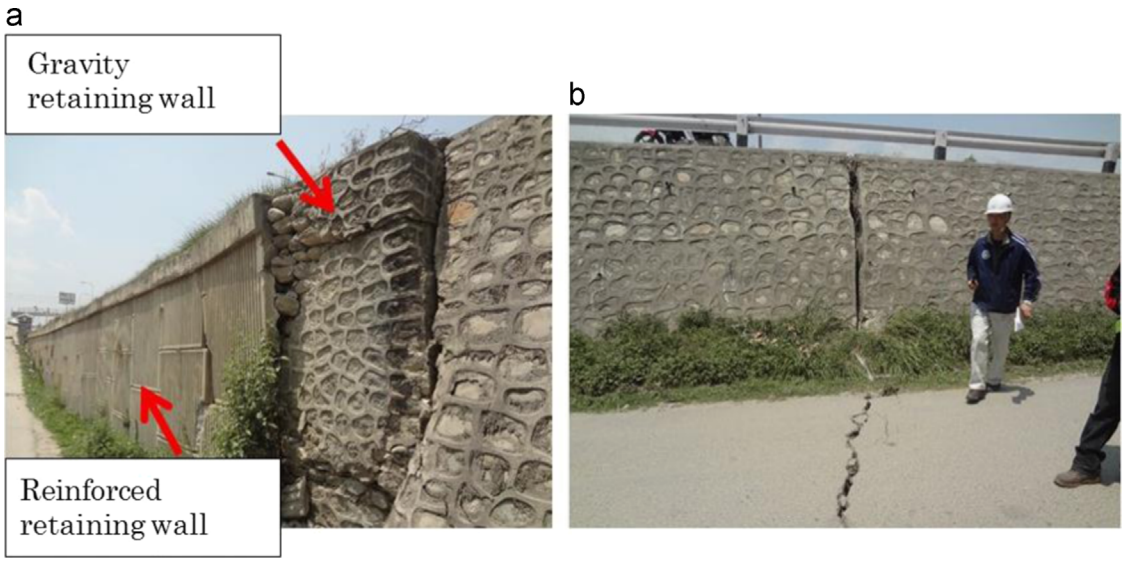

Fig. 27. Retaining wall damage and ground fissuring. (a) Damage to gravity retaining wall and (b) ground cracks.

Fig. 28. Settlement and tilting of buildings resulting from ground fissuring.

as seen from the picture. Many ground fissuring were also observed in the area surrounding the two buildings.

7. Conclusions

Following the 2015 Gorkha earthquake, the authors conducted an extensive survey in the Kathmandu valley from May 1 to 7, 2015. The results obtained are summarized as follows:

- Using the database system established by Bhandary et al. (2012), a deep soil profile up to 600 m in a NS cross section was constructed. It showed that sand and gravel deposits are dominant in the north and clay layers tend to be thicker in the south.
- A shallow soil profile up to 30 m in a east–west section showed some significant geotechnical characteristics including that the shallow soils mostly consist of sand, silt, clay, and their mixture, with a shallow ground water table, typically 1–3 m below the ground surface, and that SPT N values are mostly lower than 30.
- In order to study the correlation between the damage ratio of buildings and predominant period of ground vibration, our team carried out a partial exhaustive type survey along a NS line where microtremor measurements had been previously conducted in 2008. The predominant period of ground vibration was short at the edge of the valley and long at its center, ranging between 1.2 and 4.5 s.
- A total of 532 buildings were assessed and more than 90% of them were classified as “no damage” or “negligible to slight damage” (Grade 0 or Grade 1) while only approximately 5% of the buildings were classified as “substantial to heavy damage” to “destruction” (Grades 3–5).
- Five locations were identified where the liquefaction of soils had occurred. Liquefaction-induced damage to structures in these locations was not found, except in the case of the Nepal Engineering College where minor settlement of the college building was observed. X-ray diffraction analyses of sands erupted at liquefaction sites showed that quartz, feldspar, mica and calcite are the dominant minerals.
- During the 1934 earthquake foundation liquefaction in Tundhikhel area was observed but during the 2015 earthquake, no evidences of liquefaction were observed in this area.
- The Kathmandu–Bhaktapur Road of Araniko Highway was heavily damaged in the Lokanthali area. Heaving and subsidence of the road, slope failures in the main carriageway and access road, ground fissuring, retaining wall damage and damage to the residential buildings close to the access road were observed. Subsidence of the soft soils and their lateral spreading in this area may have exacerbated the damage to this road.

Acknowledgments

The authors would like to express their sincere thanks to Mrs. Sijapati Sweata, Mr. Deepak Bikram and KC Umesh for their great assistance during the field survey.

References

Ambraseys, N., Douglas, J., 2004. Magnitude calibration of north Indian earthquakes. Geophys. J. Int. 159 (1), 165–206.

Banerjee, P., Bürgmann, R., 2002. Convergence across the northwest Himalaya from GPS measurements. Geophys. Res. Lett. 29, 3.

Bhandary, N.P., Yatabe, R., Paudyal, Y.R., Yamamoto, K., Lohani, T.N., Dahal, R.K., 2012. Geo-info database and microtremor survey for earthquake disaster risk mitigation in Kathmandu Valley. In: Proceedings of the AWAM International Conference on Civil Engineering (AICEE'12) and Geohazard Information Zonation (GIZ'12). Malaysia (Penang). 28–30 August 2012, pp. 860–868.

Bettinelli, P., Avouac, J.P., Flouzat, M., Jouanne, F., Bollinger, L., Willis, P., Chitraker, G.R., 2006. Plate motion of India and interseismic strain in the Nepal Himalaya from GPS and DORIS measurements. J. Geodyn. 80, 567–589.

Bilham, R., Szeliga, W., 2008. Interaction Between the Himalaya and the flexed Indian plate-spatial fluctuations in seismic hazard in India in the past millennium? In: Santini, A., Moraci, N. (Eds.), Seismic Engineering Conference Commemorating the 1908 Messina and Reggio Calabria Earthquake. American Institute of Physics Conference Proceedings. pp. 224–231.

Bilham, R., Bodin, P., Jackson, M., 1995. Entertaining a great earthquake in western Nepal: historic inactivity and geodetic tests for the present state of strain. J. Nepal Geol. Soc. 11 (1), 73–78.

Chander, R., 1988. Interpretation of observed ground level changes due to the 1905 Kangra earthquake, northwest Himalaya. Tectonophysics 149, 289–298.

Chander, R., 1989. Southern limits of major earthquake ruptures along the Himalaya between longitudes 75° and 90°E. Tectonophysics 170, 115–123.

Dunn, J.A., Auden, J.B., Gosh, A.M.N., Roy, S.C., 1939. The Bihar-Nepal earthquake of 1934. Mem. Geol. Surv. India 73, 391.

GoN, 2015. Nepal Disaster Risk Reduction Portal.

European Seismological Commission, 1998. European Macroseismic Scale 1998 (EMS-98), G. Grünthal (Ed.), Centre Européen de Géodynamique et de Séismologie, Luxembourg.

GoN, 1994. Nepal National Building Code NBC 105:1994– Seismic Design of Buildings in Nepal.

Hough, S.E., Bilham, R., 2008. Site response of the Ganges basin inferred from re-evaluated macroseismic observations from the 1897 Shillong, 1905 Kangra, and 1934 Nepal earthquakes. J. Earth Syst. Sci. 117 (S2), 773–782.

JICA (Japan International cooperation Agency), 2002. The Study of Earthquake Disaster Mitigation in Kathmandu Valley. Kingdom of Nepal, Final Report, vols. I, II, III, and IV.

JICA (Japan International cooperation Agency), 2007. Planning for Improvement of Kathmandu–Bhaktapur Road in the Kingdom of Nepal, Report on the Preliminary Design and Investigation.

Khattri, K.N., 1987. Great earthquakes, seismicity gaps and potential for earthquake disaster along the Himalaya Plate boundary. Tectonophysics 138, 79–92.

Khattri, K.N., 1992. Seismic hazard in Indian Region, in Seismology in India. Curr. Sci. 62, 109–116.

Kukidome, T., Mori, S., Bhandary, N.P., 2009. Distribution of predominant period of ground across Kathmandu Valley based on microtremor measurement. In: Proceedings of the 44th Annual Conference of Japanese Geotechnical Society. pp. 1543–1544 (in Japanese).

MoHA, DPNet Nepal, UNDP, Oxfam, 2009. Nepal Disaster Report: The hazardscape and Vulnerability. Jagadamba Press. p. 116. ⟨http://www.np.undp.org/content/nepal/en/home/library/crisis_prevention_and_recovery/⟩.

Molnar, P., 1990. A review of the seismicity and the rates of active underthrusting and te deformatation at the Himalaya. J. Himal. Geol. 1, 131–154.

Molnar, P., Pandey, M.R., 1989. Rupture zones of great earthquakes in the Himalayan Region. Proc. Ind. Acad. Sci. (Earth Plant. Sci.) 98, 61–70.

NSET, GHI, 1999. National Society for Earthquake Technology—Nepal (NSET-Nepal) and GeoHazards International (GHI) Management Project. Earthquake Scenario, Product of the Kathmandu Valley Earthquake Risk.

Pandey, M.R., Molnar, P., 1988. The distribution of intensity of the Bihar–Nepal earthquake 15 January 1934 and bounds of the extent of the rupture zone. J. Nepal Geol. Soc. 5, 22–44.

Pandey, M.R., Tandukar, R.P., Avouac, J.P., Lavé, J., Massot, J.P., 1995. Interseismic strain accumulation on the Himalayan crustal ramp (Nepal). Geophys. Res. Lett. 22 (7), 751–754.

Rana, B.J.B., 1935. Nepal Ko Maha Bhukampa (Great Earthquake of Nepal). Jorganesh Press.

Sakai, H., 2001. Stratigraphic division and sedimentary facies of the Kathmandu Basin Group, central Nepal. J. Nepal Geol. Soc. 25, 19–32 (special issue).

Seeber, L., Armbruster, J.G., Quittmeyer, R.C., 1981. Seismicity and continental subduction in the Himalayan arc, in Zagros, Hindu-Kush, Himalaya, Geodynamic Evolution. Geodyn. Ser. 3, 215–242.

Seeber, L., Armbruster, J., 1981. Great detachment earthquakes along the Himalaya arc and long-term forecasting in earthquake prediction: an international review. Maurice Ewing Ser. 4, 259–279.

UNDP/HMG/UNCHS (Habitt), 1994. Seismic hazard Mapping and Risk Assessment for Nepal.

USGS, 2011. Magnitude 6.9 India–Nepal Border Region Earthquake. ⟨http://earthquake.usgs.gov/earthquakes/eqinthenews/2011/usc0005wg6/⟩.